

CFD Analysis of Flow through Single and Multi Stage Eccentric Orifice Plate Assemblies

Yashvanth S V^{*1}, Dr. V Seshadri², Yogesh Kumar K J³

^{*1}M. Tech. Student, Thermal Power Engineering, MIT-Mysore, Karnataka, India
yashvanthsvenkatesh@gmail.com¹

²Professor (Emeritus), Department of Mechanical Engineering, MIT-Mysore, Karnataka, India
dr_vseshadri@hotmail.com²

³Assistant Professor, Department of Mechanical Engineering, MIT-Mysore, Karnataka, India
yogesh_nie21@yahoo.com³

ABSTRACT

Multistage orifice plate assemblies are used as pressure reduction devices in many industrial applications. They have the advantage in the sense that, they are more compact, less noisy and have no moving parts. As compared to valves, higher pressure reductions can be obtained by these devices without choking. The design of such devices at present is based on empirical correlations derived from experience. It is usual to assume a constant discharge coefficient for all stages during the initial design. In the present work, CFD has been used to analyze the flow through multistage eccentric orifice plate assemblies and thus make the design procedure more accurate. The commercially available software package ANSYS FLUENT is used for the flow analysis. The fluid is assumed to be incompressible and Newtonian as well as flow is assumed to be steady and three dimensional. The CFD methodology has been validated by analyzing the flow through a standard concentric orifice plate assembly having diameter ratio of 0.5. The computed values of discharge coefficient and permanent pressure loss coefficient are in excellent agreement with the values given in ISO-5167 [1]. The validated methodology is used for the analysis of flow through eccentric orifice plate. Computations have been made for wide range of parameters like Reynolds number (1 to 10^6), diameter ratio (0.25 to 0.8). The computed values of discharge coefficient and permanent pressure loss coefficient agreed very well with the values given in BS-1042 [2] as long as the various flow parameters are within the range specified in the code. Data has also been generated for the eccentric orifice plate assembly, when the parameters are outside the range. CFD analyses have been carried out for multistage orifice plate assemblies with number of stages as 2, 3, 5 and 7. Each stage consisted of eccentric orifice plate having same diameter ratio with successive stages being staggered. The spacing between the stages (X/D) is varied as 0.5, 1, 2, 3, 4 and 5. Analyses have been made with two diameter ratios namely 0.3 and 0.5, Reynolds number is fixed as 10^5 . Discharge coefficient of each stage and overall permanent pressure reduction, permanent pressure loss have been computed. Conclusions on the optimum spacing, value of discharge coefficient as well as pressure reduction ratio are drawn based on the CFD analyses.

Keywords: Computational Fluid Dynamics, Eccentric Orifice Plate, Multistage Orifice plate Assembly, Discharge Coefficient, Permanent Pressure loss Coefficient, Efficiency Factor, Pressure Reduction Ratio.

I. INTRODUCTION

Orifice meter can be either used for measuring the flow rate or for restricting the flow. A typical orifice meter can be constructed by inserting a flat plate, called orifice plate, having a hole, called orifice, between two flanges of a pipe. Orifice plates can be classified on the basis of their shape, size and also on the basis of discharge conditions, shape of the upstream orifice edge and position of orifice with respect to axis of the pipe [1].

A. Eccentric Orifice Plate

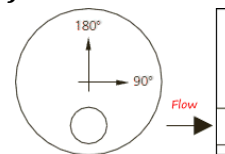


Figure.1.1: Eccentric Orifice Plate

Eccentric orifice plates are those in which the axis of the pipe and the axis of the orifice hole are not collinear as shown in the Fig. 1.1. These orifice plates are used for

measuring flow rates in two phase fluids, dusty/sediment laden fluids so that the problem of solid deposition is avoided. Further, these orifice plates are also used in pressure reduction devices like multistage orifice plate assemblies. It is normal practice to keep the bottom of the orifice plate in line with the bottom surface of the pipe to avoid accumulation of solids.

B. Multistage Orifice Plate Assemblies

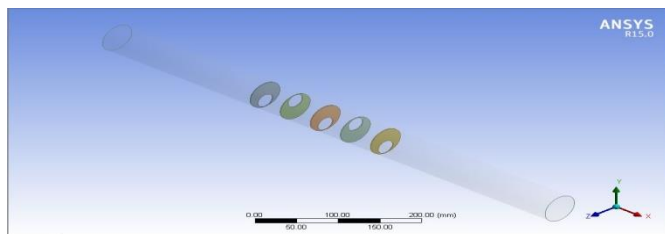


Figure.1.2: Multi stage eccentric orifice plate assembly

Multi stage eccentric orifice assemblies are used as pressure reduction devices in several industrial applications like gas blow-down, gas blow-up, cooling water recycling lines, chemical and petro chemical industries and power production plants. As compared to valves, these devices have advantages in the sense that they have no moving parts, compactness, less noisy and vibration as well as less prone to choking. The number of stages would vary depending on the pressure reduction desired and it could be as many as 10 to 12 stages. These assemblies consist of multiple stages of single-hole or multi-hole eccentric orifice plates which are staggered to achieve maximum pressure reduction.

The design of multistage eccentric orifice plate assemblies is mostly empirical with the assumption that discharge coefficient is constant for each stage and moreover number of stages used and spacing between the stages are based on experience. However, these assumptions are not strictly valid and hence there is a need to make the design procedure more scientific and accurate.

Thus the motivation in the present study is to use CFD as a tool for accurate design of the multistage eccentric orifice plate assemblies. The final goal is to use this methodology to optimise the design by choosing optimum values of various parameters like diameter ratio, number of stages and spacing between the stages so as to achieve desired pressure reduction at the existing Reynolds number.

II. LITERATURE REVIEW

A. Review of Previous Work

The analysis of flow through an eccentric orifice assembly is highly complicated since the flow is not axisymmetric and is turbulent and three dimensional. Further flow can be either steady or unsteady. In addition to this, fluid can be either compressible or incompressible with or without the influence of heat transfer. Hence only few researches have been made to analyse the flow parameters. Because of the tremendous developments in various techniques associated with CFD methodology, it has been possible to analyse any of the flow characteristics both qualitatively and quantitatively. In the present literature survey, the previous works on flow analysis through various types of orifice plate assemblies are reviewed.

Singh et al [3] carried out CFD analysis in order to evaluate the performance of orifice plates in turbulent flows under non-standard conditions. From their study, they concluded that, value of discharge coefficient (C_d) is maximum at lower Reynolds numbers and reduces slightly with increase in Reynolds number up to the range of 1.0×10^5 , thereafter effect of Reynolds number on discharge coefficient is not appreciable.

Karthik et al [4] studied the performance of orifice plates by considering the specifications outside the range specified by ISO 5167 [1]. From their CFD analysis with non-standard operating conditions, they concluded that, discharge coefficient is independent of plate thickness (E) up to 5 mm and thereafter discharge coefficient increases with increasing the plate thickness with significant deviations.

Abdulrazaq A Araoye et al [5] qualitatively analysed the characteristics when an additional orifice plate is added in a pipeline using CFD by varying the flow velocity, spacing between the orifice with a diameter ratio of $\beta=0.63$. From their qualitative analysis they concluded that, flow characteristics at the downstream of both multiple orifice plate arrangement and single orifice plate arrangement are qualitatively similar in terms of existence of shear layer region, recirculation zone and reattachment zone.

Mohan Kumar et al [6] carried out CFD analysis of flow through dual orifice plate assemblies. From their CFD analysis they concluded that, spacing between the orifice plates significantly affects the pressure reduction and the orifice plates must be placed closer to make multi stage assemblies more compact.

Lakshmisha et al [7] carried out numerical analysis on multi-stage orifice assemblies having alternate concentric and annular orifice plates. From their analysis, they concluded that, for single orifice plate, discharge coefficient (C_d) is relatively higher for annular orifice plate compared to concentric orifice plate at higher diameter ratios and vice versa at lower diameter ratios. For multi-stage assemblies, with increasing the spacing, pressure drop decreases and the optimum spacing is $X/D=1$.

Zahariea et al [8] qualitatively studied the eccentric orifice plate in comparison with classical concentric orifice plate using CFD, focusing on sedimentation tendency of the solid particles present in fluid medium whose flow rate has to be measured. By analysing streamlines they came to conclusion that, for concentric orifice plate, there exists two separated circumferential flow regions upstream and downstream the orifice plate.

Andrej Lipej et al [9] carried out research on existing orifice FWRO-004 present in feed water recirculation line of NPP krsko in the view of hydraulic analysis and design of a new multi-stage multi-hole orifice plate assemblies in order to minimize the cavitation, vibrations and high pressure pulsations in the pipeline. From the numerical analysis, they concluded that by using multi-stage orifice plates pressure can reduced to greater extent and higher pressure drop occurs at the first and the lower pressure drop occurs at the last stage to avoid cavitation.

B. Scope of Present Study

The objectives of the present study are as follows,

- To develop CFD methodology for analyzing flow through single stage and multi stage eccentric orifice plate assemblies (viz. choice of suitable turbulence model, meshing technique, discretization technique etc.)
- Analysis of flow through single stage eccentric orifice plate for studying the effect of different diameter ratios and Reynolds numbers on discharge

coefficient and permanent pressure loss coefficient. The effect of plate thickness as well as pipe roughness on the characteristics of the eccentric orifice plate.

- Analysis of flow through multi stage eccentric orifice plate assemblies as a function of spacing between the stages, diameter ratio and number of stages. Quantitative data on the optimum values for the various design parameters is proposed to be generated.

III. CFD METHODOLOGY AND VALIDATION

A. Methodology

Methodology is the step by step sequence of operations followed for the analysis of the given problem. The numerical analysis of any of the flow mainly involves the approximation of the problem geometry, choosing appropriate mathematical model, selection of proper discretization technique, solving with suitable boundary conditions and analysing the solution for various flow characteristics. In this present study, Numerical simulations are carried out using the commercially available CFD software package ANSYS workbench 15.0 with finite volume approximations.

B. Validation

Validation is the first and foremost essential step in the numerical analysis of any flow. It is nothing but process of comparing the results obtained using CFD with the available standard results, so as to ensure that the methodology followed is suitable for the particular type of problem.

C. Turbulent Flow of Incompressible Fluid through a Standard Concentric Orifice Plate

In the present study, validation is carried out on Turbulent flow of incompressible fluid through a standard concentric orifice plate. The obtained CFD results are compared with the standard values given in ISO 5167-1:1991 [1].

Modelling

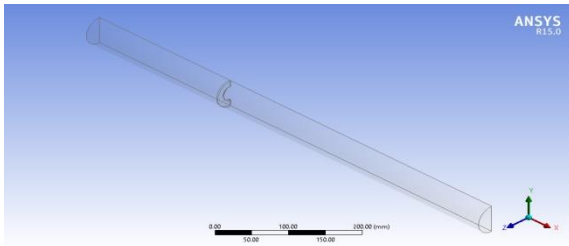


Figure.3.1: Geometry of Standard concentric orifice plate

The concentric orifice plate geometry was modelled using ANSYS Design modeller, since the flow is symmetric about the mid vertical plane (XY-plane), symmetric geometry is modelled with orifice diameter =25 mm, diameter ratio =0.5, thickness of orifice plate = 2.5mm, thickness of orifice = 1mm, angle of bevel = 45° , upstream and downstream lengths of 5D and 10D respectively inserted in a pipe of diameter 50mm. The properties of fluid considered are, free stream velocity = 2m/s, density = 1000kg/m^3 , viscosity = 0.001 Pa-s and $Re_D = 10^5$.

Meshing

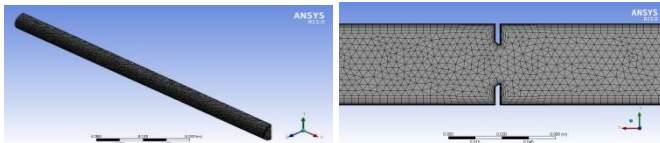


Figure.3.2: Mesh used for Standard concentric orifice plate

Meshing was done using ANSYS Meshing tool, The mesh was structured with 3D tetrahedron elements using program controlled inflation meshing having wall y^+ values in the range of unity, growth rate in the range of 1.2 to 1.4 with the first layer thickness corresponding to the Reynolds number and maximum number of layers in the range of 10 to 15. Mesh consists of 144306 nodes and 349717 elements and is as shown in Fig. 3.2.

Boundary conditions

The different boundaries of the geometry are given with suitable boundary conditions as follows. Velocity-inlet boundary condition is provided at the inlet with the magnitude of 2 m/s, pressure-outlet boundary condition is provided at the outlet with the gauge pressure $p_g = 0$, mid vertical symmetrical plane is given as symmetry and wall is taken as smooth wall with stationary and no slip boundary condition.

Solving

The present problem was solved using ANSYS FLUENT parallel solver for different turbulence models. Steady state pressure based solver was used with SIMPLE algorithm for pressure-velocity coupling, Green-Gauss node based method for gradient, with turbulent intensity and hydraulic diameter specification methods were used. The solution absolute convergence criterion is taken as 10^{-6} .

Design Specifications for Standard Concentric Orifice Plate

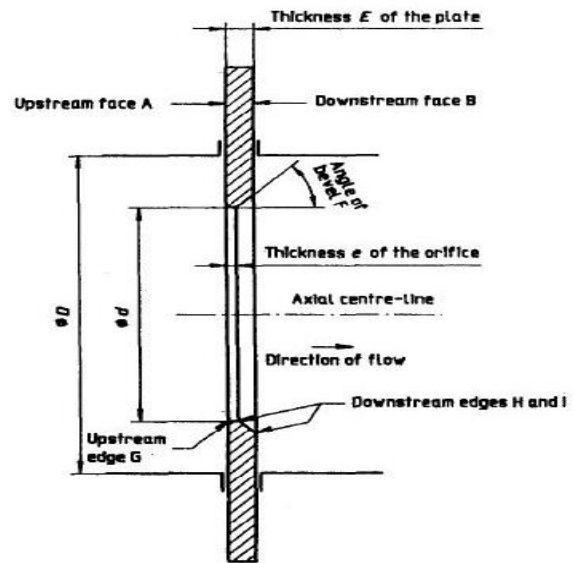


Figure.3.3: Design Specifications for Standard Orifice Plate

As per ISO 5167-1[1], the standard concentric orifice plate can be used only within the range specified as follows,

- Diameter of the pipe (D) shall be within the range 50 mm to 1000 mm.
- Diameter of the orifice (d) shall be greater than or equal to 12.5 mm.
- Diameter ratio (β) shall be within the range 0.1 to 0.75.
- Thickness 'e' of the orifice shall be within the range $0.0005D$ to $0.02D$.
- Thickness 'E' of the orifice plate shall be in the range of 'e' to $0.05D$. But, when $50\text{ mm} < D < 64\text{ mm}$, an orifice plate with thickness of up to 3.2 mm can be used.
- Angle of bevel (F or α) shall be $45^{\circ} \pm 15^{\circ}$.

These pressure tapings have to be in accordance with ISO 5167 [1]. The choice pressure taps can be D & D/2, corner taps, flange taps etc. The restrictions on parameters like β , Re_D , D etc. are given in the standards for each arrangements of pressure taps [1].

Discharge Coefficient

The actual mass flow rate through an orifice is given by,

$$Q_m = \frac{C_d F_\alpha \epsilon F_E}{\sqrt{1 - \beta^4}} \times \frac{\pi D^2}{4} \times \sqrt{2 \Delta p \rho}$$

Where,

Q_m = Mass flow rate (kg/s)

C_d = Discharge Coefficient

F_α = Correction factor for thermal expansion

ϵ = Expansibility factor

F_E = Roughness correction factor

D = Diameter of pipe (m)

d = Diameter of orifice (m)

$\beta = d/D$ = Diameter ratio

ΔP = Pressure drop (Pa)

ρ = Density of the fluid (kg/m³)

If the fluid is assumed to be incompressible then $\epsilon = 1$, if measurements are done in normal temperature then $F_\alpha = 1$ and if the pipe surface is assumed to be smooth then roughness correction factor $F_E = 1$.

By applying the above assumptions, the modified equation for mass flow rate is given by,

$$Q_m = \frac{C_d}{\sqrt{1 - \beta^4}} \times \frac{\pi D^2}{4} \times \sqrt{2 \Delta p \rho}$$

Discharge coefficient (C_d) can be defined as the ratio of actual discharge to theoretical discharge. Value of C_d is always less than unity due to the occurrence of losses in the actual case and is given by the equation,

$$C_d = \frac{Q_m \sqrt{1 - \beta^4}}{\frac{\pi D^2}{4} \sqrt{2 \Delta p \rho}}$$

As per ISO-5167 [1], the discharge coefficient (C_d) for an standard concentric orifice plate is given by Reader-Harris/Gallagher equation and is given by,

$$C_d = 0.5961 + 0.0261\beta^2 - 0.216\beta^8 + 0.000521 \left(\frac{10^6 \beta}{Re_D} \right)^{0.7} + (0.0188 + 0.0063A)\beta^{3.5} \left(\frac{10^6}{Re_D} \right)^{0.3} + (0.043 + 0.08e^{-10L_1} - 0.123e^{-7L_1})(1 - 0.11A) \left(\frac{\beta^4}{1 - \beta^4} \right) - 0.031(M'_2 - 0.8M'_2)^{1.1} \beta^{1.3}$$

Where,

C_d = Discharge coefficient

D = Diameter of pipe (m)

d = Diameter of orifice (m)

$\beta = d/D$ = Diameter ratio

Re_D = Reynolds number related to D

$$A = \left(\frac{19000\beta}{Re_D} \right)^{0.8}$$

$$M'_2 = \frac{2L'_2}{1 - \beta}$$

$L_1 = L'_1/D$ = Quotient of distance between upstream tapping and upstream face of the plate

$L'_2 = L'_2/D$ = Quotient of distance between downstream tapping and downstream face of the plate

For flange tappings, $L_1 = L'_2 =$

$$\frac{25.4}{D} \text{ (where, } D \text{ is in mm)}$$

For corner tapping, $L_1 = L'_2 = 0$

For D and $D/2$ tappings, $L_1 = 1$ and $L'_2 = 0.47$

Uncertainties in Discharge Coefficient

For all three specified types of pressure tappings with the values of β , D , Re_D and (Ks/D) are assumed to be known without error, then the relative uncertainty in the value of discharge coefficient given by ISO 5167-1 [1] (Reader-Harris/Gallagher equation) is equal to

$$0.5 \% \text{ for } \beta \leq 0.6$$

$$(1.667\beta - 0.5) \% \text{ for } 0.6 \leq \beta \leq 0.75$$

Permanent Pressure Loss

When the fluid is made to flow through a pipe, due to the friction between the fluid and wall surface pressure losses occurs, this pressure loss is a measure of energy loss due to the introduction of orifice and is considered as permanent pressure loss (ΔP_{perm}).

As per ISO-5167 [1], (ΔP_{perm}) is given by,

$$\Delta p_{perm} = \frac{\sqrt{1 - \beta^4} - C_d \beta^2}{\sqrt{1 - \beta^4} + C_d \beta^2} \Delta p$$

But the actual permanent pressure loss for an orifice meter can be defined as the “difference in pressure drop of the fluid between inlet and outlet of pipe with orifice and without an orifice, under same flow conditions”.

Actual permanent pressure loss is given by,

$$\Delta p_{perm} = \Delta p' - \Delta p''$$

Where,

(ΔP_{perm}) = Permanent pressure loss (Pa)

ΔP = Pressure drop across orifice plate (Pa)

$\Delta P'$ = Pressure drop between inlet and outlet of pipe with orifice (Pa)

$\Delta P''$ = Pressure drop between inlet and outlet of pipe without orifice (Pa)

Permanent pressure loss coefficient (C_L)

Permanent pressure loss coefficient (C_L) can be defined as the ratio of permanent pressure loss (ΔP_{perm}) to the pressure drop across the orifice plate (ΔP) and is given by,

$$C_L = \frac{(\Delta P)_{perm}}{\Delta P}$$

Results and Discussion

The comparison of ISO 5167 [1] standard results and CFD results for different turbulence models are tabulated in the Table. 3.1.

Turbulence Model	ΔP (Pa)	$(C_d)_{ISO}$	$(C_d)_{CFD}$	$(C_L)_{ISO}$	$(C_L)_{CFD}$
k-ϵ Standard	81207	0.6082	0.6078	0.7285	0.7523
k-ϵ RNG	80867	0.6082	0.6090	0.7285	0.7633
k-ϵ Realizable	82613	0.6082	0.6026	0.7285	0.7401
k-ω Standard	78149	0.6082	0.6195	0.7285	0.7717
k-ω SST	79545	0.6082	0.6141	0.7285	0.7691

The results obtained from k- ϵ Standard turbulence model are in very close agreement with the ISO 5167 [1] standard results. Hence the CFD methodology used for the standard concentric orifice plate is validated.

Conclusions

From the CFD methodology and validation discussed in this section, it can concluded that,

- The mesh has to be structured with 3D tetrahedron elements using program controlled inflation meshing having wall y^+ values in the range of unity (at the chosen Reynolds number), growth rate in

the range of 1.2 to 1.4 with maximum number of inflation layers in the range of 10 to 15.

- Number of elements should be maintained in the range or above 3.0×10^5 to 3.5×10^5 for the accuracy of results.
- K- ϵ Standard turbulence model (scalable wall function) with turbulent intensity and hydraulic diameter specification method using Green-Gauss Node based gradient method was found to be most suited for this class of flows.
- Absolute convergence criteria of 10^{-6} must be provided for residuals to ensure computational accuracy.

IV. ANALYSIS OF FLOW THROUGH SINGLE STAGE ECCENTRIC ORIFICE PLATE

In this section, turbulent flow of incompressible fluid through an eccentric orifice plate is considered for the analysis. The results obtained from computations are compared with the Codal values of BS 1042 [2].

Modelling and Flow Domain

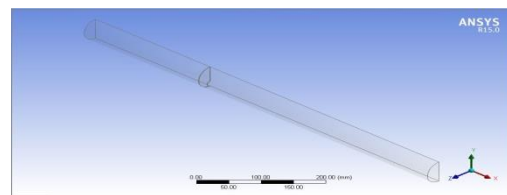


Figure.4.1: Geometry of eccentric orifice plate

Since the flow is symmetric about the mid vertical plane (XY- plane) only half of the domain is modelled with pipe diameter (d) = 50 mm, thickness of orifice plate (E) = 1 mm without bevelling, upstream and downstream lengths of 5D and 10D respectively. Different geometries are modelled with different diameter ratios $\beta = 0.25, 0.35, 0.45, 0.5, 0.6$ and 0.8 . The properties of fluid considered are free stream velocity = 2m/s, density = 1000 kg/m³, Reynolds number in the range 1 to 10⁶ and viscosities are calculated as per the Reynolds number considered.

Meshing

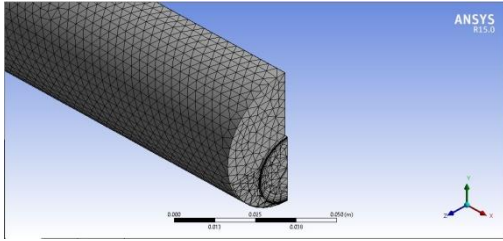


Figure.4.2: Isometric view of the Mesh in the Cross Section near the Orifice

The size of the wall adjacent cells or thickness of first layer ‘y’ (in meters) is calculated in accordance with the chosen Reynolds number using the law of wall [11].

The non-dimensional distance from wall (y^+) is given by,

$$y^+ = \frac{y U_0^*}{\nu}$$

Where,

$$\frac{U_0^*}{U_{Avg}} = \sqrt{\frac{f}{8}}$$

$$\text{Friction factor, } f = \frac{0.316}{Re_D^{0.25}}$$

$$\text{Kinematic viscosity, } \nu = \frac{\mu}{\rho}$$

By substituting the above terms in y^+ equation, we get,

$$y^+ = y U_{Avg} \sqrt{\frac{0.316}{8 \times Re_D^{0.25}}} \frac{\rho}{\mu}$$

Therefore, from the above equation, the first layer thickness (in meters) is given by,

$$y = \frac{y^+ \mu}{\rho U_{Avg} \sqrt{\frac{0.316}{8 \times Re_D^{0.25}}}}$$

Thus, mesh at the wall has to be either very fine enough or coarse to avoid the placing of wall adjacent cells in the buffer layer ($5 < y^+ < 30$).

Hence, if the values of Reynolds number, density, viscosity and velocity of the fluid are known then the value of first layer thickness (in meters) can be calculated by choosing the value of y^+ not in the range $5 < y^+ < 30$. Usually, y^+ is chosen in the range of unity (say $y^+ = 0.9$) for ensuring the accuracy of computations. Thus, mesh near the wall has to be very fine.

Boundary Conditions

The different boundaries of the geometry are given with suitable boundary conditions as follows. Velocity-inlet boundary condition is provided at the inlet with the magnitude of 2 m/s, pressure-outlet boundary condition is provided at the outlet with the gauge pressure $P_g = 0$, mid vertical symmetrical plane is given as symmetry and wall is taken as smooth wall with stationary and no slip boundary condition.

Design Specifications for Eccentric Orifice Plate

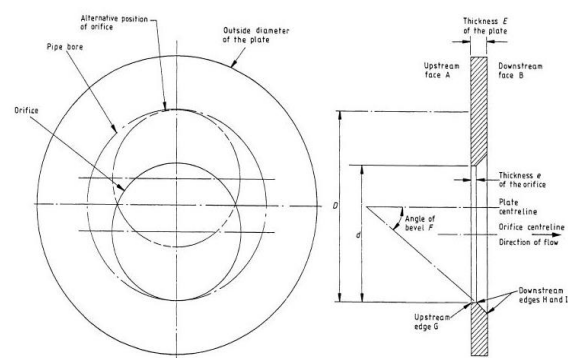


Figure.4.3: Design Specifications for Eccentric Orifice Plate

As per BS 1042 [2], the range of limits of use for an eccentric orifice plate are specified as follows,

$$\begin{aligned} d &> 50 \text{ mm} \\ 100 \text{ mm} &< D < 1000 \text{ mm} \\ 0.46 &< \beta < 0.84 \\ 0.136 &< C\beta^2(1-\beta^4)^{0.5} < 0.423 \\ 2 \times 10^5 \beta^2 &< Re_D < 10^6 \beta \end{aligned}$$

- Thickness ‘e’ of the orifice shall be within the range 0.0005D to 0.02D.
- Thickness ‘E’ of the orifice plate shall be in the range of ‘e’ to 0.05D.
- If the thickness of the orifice plate ‘E’ is greater than the thickness of the orifice ‘e’, orifice plate must be beveled on the downstream face with an bevel angle (F or α) of $45^\circ \pm 15^\circ$.
- If the thickness of the orifice plate ‘E’ is less than or equal to 0.02D, then the plate shall not be beveled.

Pressure Tappings for Eccentric Orifice Plate

Eccentric orifice plate must be provided with a pair of corner tappings at a distance ‘a’ within the range

3 mm < a < 10 mm diametrically opposite to the orifice hole.

Discharge Coefficient

As per BS 1042 [2], the discharge coefficient (C_d) for an eccentric orifice plate is given by the equation,

$$C_d = 0.9355 - 1.6889\beta + 3.0428\beta^2 - 1.7989\beta^3$$

Where,

C_d = Discharge coefficient

D = Diameter of pipe (m)

d = Diameter of orifice (m)

$\beta = d/D$ = Diameter ratio

Uncertainties in Discharge Coefficient

When the values of β , D , Re_D and (Ks/D) are assumed to be known without error, then the relative uncertainty in the value of discharge coefficient given by BS 1042 [2] is equal to,

$$1 \% \text{ when } \beta < 0.75$$

$$2 \% \text{ when } \beta > 0.75$$

If the pipe is rough, then the discharge coefficient for a smooth pipe must be multiplied with an appropriate roughness correction factor (F_E) to obtain the discharge coefficient for a rough pipe. If the pipe is assumed to be smooth, then F_E can be taken as 1.000.

Results and Discussion

A. Effect of Reynolds number and Diameter Ratio Characteristics of Eccentric Orifice Plate

Computations have been made for a wide range of parameters. The diameter ratios considered are 0.25, 0.35, 0.45, 0.5, 0.6 and 0.8, at each diameter ratio Reynolds number is varied in the range 1 to 10^6 covering both laminar and turbulent regimes. At each diameter ratio and Reynolds number, the values of discharge coefficient (C_d) and permanent pressure loss coefficient (C_L) are computed using the relationships already given and they are compared with the values given in BS 1042 [2] and the results are tabulated in the Table 4.1 (a) to 4.1 (f).

In each Table the computations corresponding to Reynolds number in the range specified by BS 1042 [2] are shown in Bold and Italic letters and the values which are not highlighted are not within the range of

applicability of BS 1042 [2]. Nevertheless they are given for the sake of completeness.

As per BS 1042, the diameter ratio has to be in the range $0.46 < \beta < 0.84$. The values of diameter ratios in Tables 4.1 (c) to 4.1 (f) are within the range, the tabulated values in these Tables shows that the computed values of discharge coefficient (C_d) are in very good agreement with the values given in BS 1042 [2] as long as Reynolds number and diameter ratios are within the range. However outside this range ($\beta = 0.25$ and 0.35), the deviations are somewhat higher and the computed values are lower than the Codal values. Further, at lower values of Reynolds number, discharge coefficient decreases with decreasing Reynolds number except when the flow is undergoing transition.

Tables 4.1 (a) to 4.1 (f) also show the computed and Codal values of permanent pressure loss coefficient. It is to be noted that the Codal values of permanent pressure coefficient are for concentric orifice plate and not for eccentric orifice plate. It is observed that, at all diameter ratios and Reynolds numbers the computed values of permanent pressure loss coefficient are higher than the Codal values. This can be attributed to enhanced dissipation of energy in the eccentric orifice plate due to the three dimensional effects on the flow downstream of the orifice plate.

The variation of discharge coefficient with Reynolds number at different diameter ratios are graphically plotted in the Figs. 4.4 (a) to 4.4 (f). It is observed that at any given diameter ratio, discharge coefficient remains more or less constant as long as Reynolds number is higher than 10^4 , then it shows increasing trend as Reynolds number decreases and finally at Reynolds number less than 100 there is a steep fall in the value of discharge coefficient due to enhanced viscous losses.

Table 4.1 (a): Effect of Re_D on characteristics of single stage eccentric orifice plate with $D = 50$ mm, $E = 1$ mm & $\beta = 0.25$					
Re_D	ΔP (Pa)	$(C_d)_{BS}$	$(C_d)_{CFD}$	$(C_L)_{BS}$	$(C_L)_{CFD}$
1	5794943	0.6753	0.2966	0.9188	0.9868
10	1325137	0.6753	0.6203	0.9188	0.9560
100	1145335	0.6753	0.6672	0.9188	0.9543
1000	1218774	0.6753	0.6468	0.9188	0.9489
12500	1259915	0.6753	0.6362	0.9188	0.9442
100000	1277020	0.6753	0.6319	0.9188	0.9417
250000	1290372	0.6753	0.6286	0.9188	0.9420
500000	1293977	0.6753	0.6278	0.9188	0.9406

Table 4.1 (b): Effect of Re_D on characteristics of single stage eccentric orifice plate with $D= 50$ mm, $E = 1$ mm & $\beta = 0.35$

Re_D	ΔP (Pa)	$(C_d)_{BS}$	$(C_d)_{CFD}$	$(C_L)_{BS}$	$(C_L)_{CFD}$
1	2059836	0.6400	0.2524	0.8535	0.9280
10	385157	0.6400	0.5838	0.8535	0.8919
100	291166	0.6400	0.6714	0.8535	0.8918
1000	300579	0.6400	0.6608	0.8535	0.8925
24500	331231	0.6400	0.6295	0.8535	0.8897
100000	335763	0.6400	0.6252	0.8535	0.8862
350000	335991	0.6400	0.6250	0.8535	0.8869
500000	338688	0.6400	0.6225	0.8535	0.8839
10^6	336614	0.6400	0.6244	0.8535	0.8871

Table 4.1 (c): Effect of Re_D on characteristics of single stage eccentric orifice plate with $D= 50$ mm, $E = 1$ mm & $\beta = 0.45$

Re_D	ΔP (Pa)	$(C_d)_{BS}$	$(C_d)_{CFD}$	$(C_L)_{BS}$	$(C_L)_{CFD}$
1	966730	0.6277	0.2199	0.7702	0.9103
10	155736	0.6277	0.5480	0.7702	0.8828
100	105464	0.6277	0.6659	0.7702	0.8158
1000	110435	0.6277	0.6507	0.7702	0.8256
40500	111033	0.6277	0.6490	0.7702	0.8152
100000	119777	0.6277	0.6249	0.7702	0.8116
450000	119816	0.6277	0.6248	0.7702	0.8121
500000	119867	0.6277	0.6246	0.7702	0.8099
10^6	119854	0.6277	0.6247	0.7702	0.8117

Table 4.1 (d): Effect of Re_D on characteristics of single stage eccentric orifice plate with $D= 50$ mm, $E = 1$ mm & $\beta = 0.45$

Re_D	ΔP (Pa)	$(C_d)_{BS}$	$(C_d)_{CFD}$	$(C_L)_{BS}$	$(C_L)_{CFD}$
1	696864	0.6268	0.2074	0.7214	0.8840
10	106508	0.6268	0.5307	0.7214	0.8045
100	67094	0.6268	0.6686	0.7214	0.7514
1000	71905	0.6268	0.6459	0.7214	0.7888
10000	73311	0.6268	0.6397	0.7214	0.7780
50000	75066	0.6268	0.6321	0.7214	0.7742
100000	76045	0.6268	0.6280	0.7214	0.7714
500000	76418	0.6268	0.6265	0.7214	0.7663
10^6	76330	0.6268	0.6269	0.7214	0.7672

Table 4.1 (e): Effect of Re_D on characteristics of single stage eccentric orifice plate with $D= 50$ mm, $E = 1$ mm & $\beta = 0.6$

Re_D	ΔP (Pa)	$(C_d)_{BS}$	$(C_d)_{CFD}$	$(C_L)_{BS}$	$(C_L)_{CFD}$
1	412349	0.6290	0.1804	0.6093	0.6294
10	57684	0.6290	0.4825	0.6093	0.5929
100	29188	0.6290	0.6783	0.6093	0.6340
1000	33357	0.6290	0.6345	0.6093	0.7029
10000	33438	0.6290	0.6338	0.6093	0.6854
72000	33928	0.6290	0.6292	0.6093	0.6707
100000	33982	0.6290	0.6287	0.6093	0.6644
600000	34080	0.6290	0.6278	0.6093	0.6662
10^6	34022	0.6290	0.6283	0.6093	0.6663

Table 4.1 (f): Effect of Re_D on characteristics of single stage eccentric orifice plate with $D= 50$ mm, $E = 1$ mm & $\beta = 0.8$

Re_D	ΔP (Pa)	$(C_d)_{BS}$	$(C_d)_{CFD}$	$(C_L)_{BS}$	$(C_L)_{CFD}$
1	175718	0.6107	0.1280	0.3256	0.5651
10	20975	0.6107	0.3707	0.3256	0.5150
100	6576	0.6107	0.6620	0.3256	0.3565
1000	7279	0.6107	0.6293	0.3256	0.4733
10000	7709	0.6107	0.6115	0.3256	0.4274
128000	7947	0.6107	0.6022	0.3256	0.4187
500000	8097	0.6107	0.5966	0.3256	0.4046
800000	8203	0.6107	0.5928	0.3256	0.4052
10^6	8194	0.6107	0.5931	0.3256	0.4011

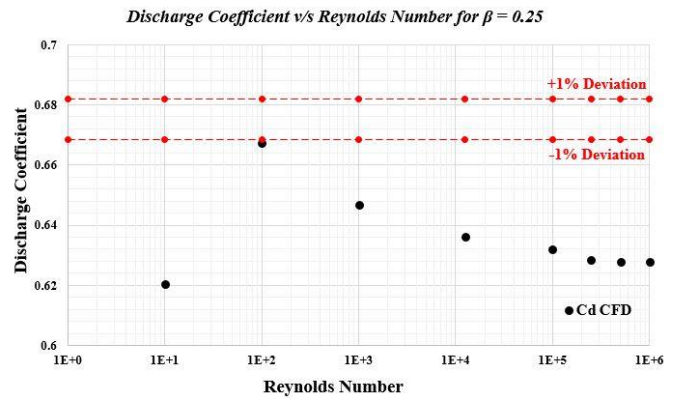


Figure.4.4 (a): Variation of C_d with Re_D having $D=50$ mm, $E=1$ mm & $\beta=0.25$

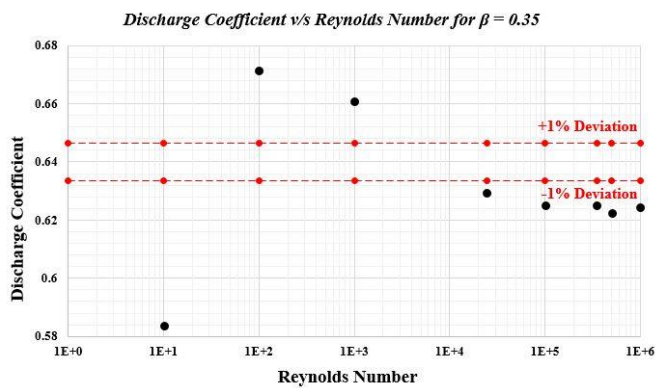


Figure.4.4 (b): Variation of C_d with Re_D having $D=50$ mm, $E=1$ mm & $\beta=0.35$

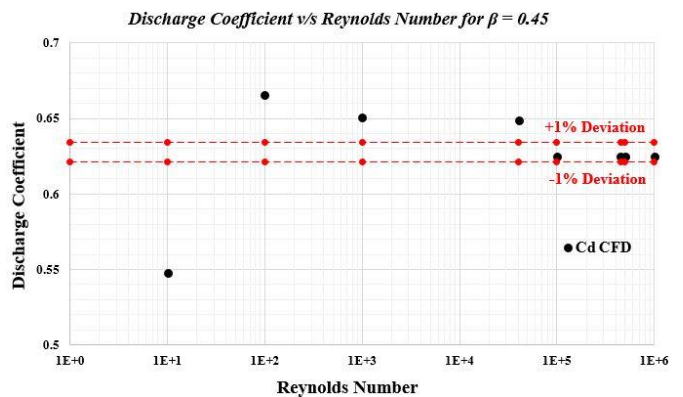


Figure.4.4 (c): Variation of C_d with Re_D having $D=50$ mm, $E=1$ mm & $\beta=0.45$

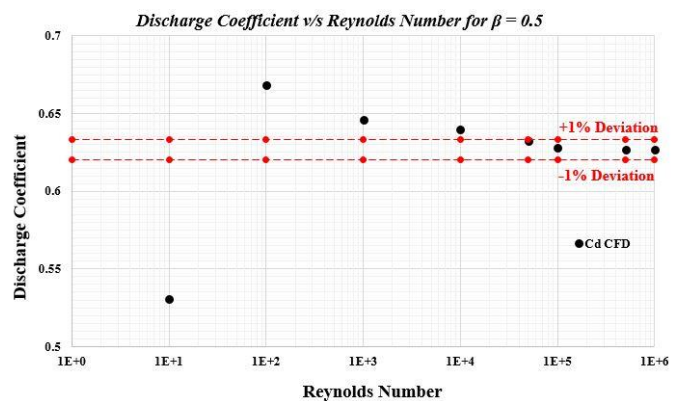


Figure.4.4 (d): Variation of C_d with Re_D having $D=50$ mm, $E=1$ mm & $\beta=0.5$

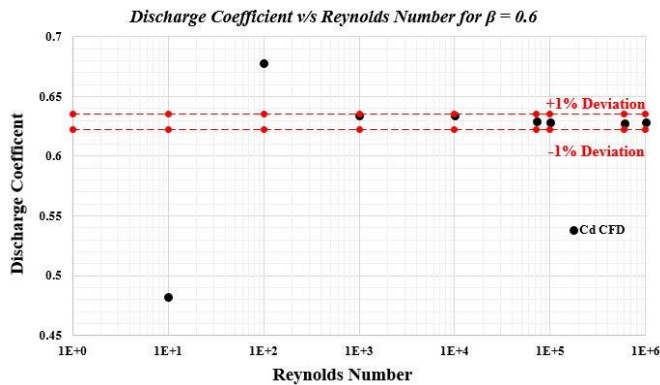


Figure.4.4 (e): Variation of Cd with Re_D having $D = 50$ mm, $E = 1$ mm & $\beta = 0.6$

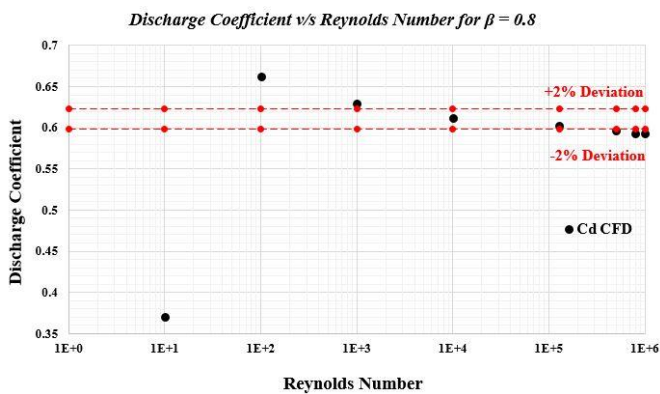


Figure.4.4 (f): Variation of Cd with Re_D having $D = 50$ mm, $E = 1$ mm & $\beta = 0.8$

B. Effect of pipe roughness on characteristics of eccentric orifice plate

Characteristics of single stage eccentric orifice plate are analysed by considering the Effect of pipe roughness with the specifications $D = 50$ mm, $Re_D = 10^5$, $E = 1$ mm & $\beta = 0.5$. Stimulations are carried by considering the relative roughness (K_s/D) in the range 0 to 5×10^{-3} . The discharge coefficient, permanent pressure loss coefficient and roughness correction factor (F_E) are calculated and compared with the standard values of BS1042 [2] as tabulated in Table. 4.2.

K_s/D	ΔP (Pa)	$(C_a)_{BS}$	$(C_a)_{CFD}$	$(C_L)_{BS}$	$(C_L)_{CFD}$	$(F_E)_{BS}$	$(F_E)_{CFD}$
0	76045	0.6268	0.6280	0.7214	0.7714	1.0000	1.0000
10^{-5}	76047	0.6268	0.6280	0.7214	0.7714	1.0000	1.0000
10^{-4}	76045	0.6268	0.6280	0.7214	0.7715	1.0000	1.0000
5×10^{-4}	75988	0.6268	0.6281	0.7214	0.7757	1.0000	1.0001
10^{-3}	76030	0.6270	0.6283	0.7214	0.7794	1.0000	1.0004
5×10^{-3}	76145	0.6312	0.6287	0.7214	0.7887	1.0071	1.0011

The results from these analysis are tabulated in the Table. 4.2. BS 1042 [2] also defines a roughness correction factor (F_E) for pipe roughness which has to be multiplied by the discharge coefficient for smooth pipe under same flow conditions to obtain the discharge

coefficient for rough pipe. The computed values of roughness correction factor (F_E) are also given in Table. 4.2. It is observed that effect of roughness is not very significant as long as relative roughness (K_s/D) is less than 10^{-4} . However, at higher relative roughness (K_s/D) there is a reduction in discharge coefficient, this conclusions are in great agreement with tabulated values of roughness correction factor (F_E) in BS 1042 [2].

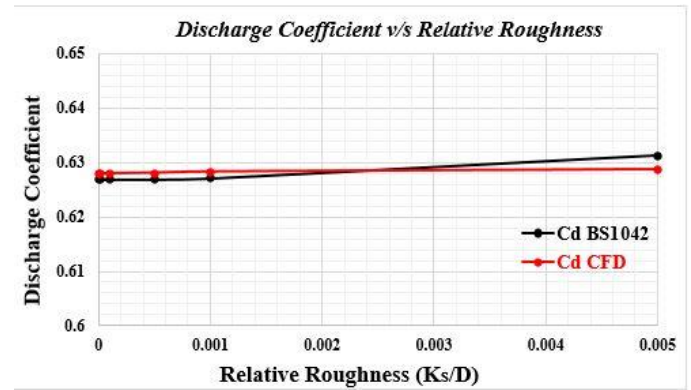


Figure. 4.5: Variation of Cd with (K_s/D) having $D = 50$ mm, $\beta = 0.5$ & $Re_D = 10^5$

C. Effect of orifice plate thickness (E) on characteristics of single stage eccentric orifice plate

As per BS 1042 [2], the maximum allowable plate thickness (E) for an eccentric orifice plate is $0.05D$. However, in many industrial applications due to the existence of very high pressure thicker orifice plate have to be used. This is particularly so when these device are used as pressure reduction devices. Hence computations have been made for various orifice plate thickness. For this analysis, the values of seven plate thickness in the range 1 mm to 7 mm are analysed, no bevelling is provided in each of these cases. For these analysis, $D = 50$ mm, $d = 25$ mm and $Re_D = 10^5$ are considered.

E (mm)	ΔP (Pa)	$(C_a)_{BS}$	$(C_a)_{CFD}$	$(C_L)_{BS}$	$(C_L)_{CFD}$
1	76045	0.6268	0.6280	0.7214	0.7714
2	73324	0.6268	0.6396	0.7214	0.7685
3	70652	0.6268	0.6516	0.7214	0.7673
4	68977	0.6268	0.6594	0.7214	0.7733
5	70264	0.6268	0.6534	0.7214	0.7700
6	70422	0.6268	0.6526	0.7214	0.7653
7	68905	0.6268	0.6598	0.7214	0.7682

The computed values of discharge coefficient and permanent pressure loss coefficient are tabulated in Table 4.3. This is to be noted that maximum allowable plate thickness (E) for this case is 2.5mm. If the plate thickness is more than 1mm, bevelling is recommended. However, in the present analysis bevelling is not provided. The computations have shown that, as the thickness of the plate (E) increases beyond 2mm, discharge coefficient also increases. However, permanent pressure loss coefficient is not significantly affected.

D. Effect of Pressure Tapping Location on Pressure Differential across Eccentric Orifice Plate

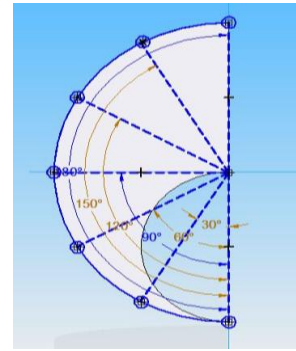


Figure.4.8: Cross Section of Eccentric Orifice Plate with Circumferential Pressure Tappings $D = 50 \text{ mm}$ & $\beta = 0.5$

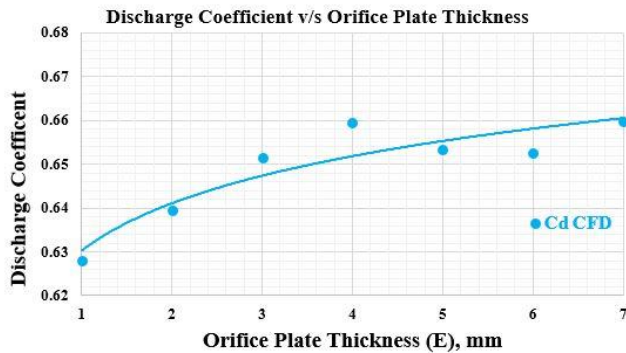


Figure.4.6: Variation of C_d with (E) having $D = 50 \text{ mm}$, $\beta = 0.5$ & $Re_D = 10^5$

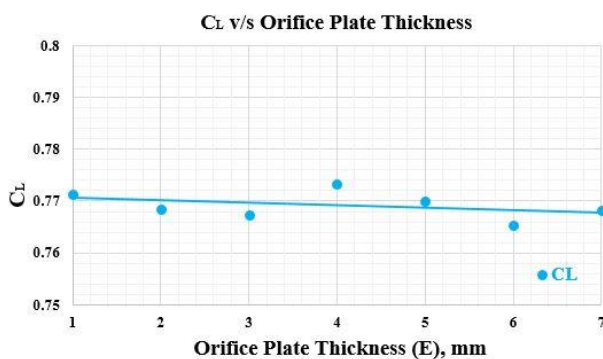


Figure.4.7: Variation of C_L with (E) having $D = 50 \text{ mm}$, $\beta = 0.5$ & $Re_D = 10^5$

Fig. 4.6 show the variation of discharge coefficient (C_d) with orifice plate thickness (E), which confirms the trend described above. Also Fig. 4.7 show the variation of permanent pressure loss coefficient (C_L) with orifice plate thickness (E), which indicates that permanent pressure loss coefficient (C_L) is unaffected by orifice plate thickness.

Since the flow is asymmetric in case of eccentric orifice plate, the pressure field on both upstream and downstream of orifice plate will be three dimensional. Hence circumferential location of pressure taps affects the measured pressure differential there by affecting discharge coefficient. In order to quantify this effect, the pressure differential across the pipe as a function of circumferential position is analysed. The angle ' θ ' is defined as shown in Fig. 4.8.

Usually the pressure taps are located at $\theta = 180^\circ$, when both upstream and downstream pressure taps are located at different angular positions, the variation in ΔP is calculated and tabulated in Table 4.4.

θ (deg)	ΔP (Pa)	$\frac{\Delta P(\theta)}{\Delta P_{\theta=180^\circ}}$
0°	25099.11	0.3300
30°	68871.09	0.9056
60°	74154.83	0.9751
90°	76100.63	1.0000
120°	76963.59	1.0120
150°	76593.64	1.0070
180°	76045.10	1.0000

It is observed that, ΔP depends on the value of ' θ ' particularly when it is less than 90° . As expected ΔP is minimum at $\theta = 0^\circ$ (bottom of the pipe).

Conclusions

The following broad conclusions are drawn from the CFD analysis of flow through eccentric orifice plates,

- The validated CFD methodology can be used to predict the values of discharge coefficient and permanent pressure loss coefficient even at the

working conditions outside the range specified by BS 1042 [2].

- As long as, the range of flow parameters are within the limits specified by BS 1042 [2], the CFD values are in good agreement with the Codal values, the deviations being within the uncertainty limits.
- If the values of Reynolds number and diameter ratio are outside the limits, CFD can still be used to calculate the values of discharge coefficient and permanent pressure loss coefficient.
- The permanent pressure loss coefficient in case of eccentric orifice plate is always higher than that of concentric orifice plate under equivalent working conditions. This is due to the non-axisymmetric flow effects.
- If the thickness of the eccentric orifice plate increases beyond the allowable limits, the value of discharge coefficient increases. However, permanent pressure loss coefficient is not significantly affected.
- In the case of rough pipe, up to relative roughness $(K_s/D) = 10^{-3}$, the effect on discharge coefficient and permanent pressure loss coefficient is not significant. Beyond that, minor effect is observed.
- For an eccentric orifice plate, corner taps must be placed as close to $\theta = 180^\circ$ as possible.
- For both concentric and eccentric orifice plates, the discharge coefficient is not a function of Reynolds number in the fully turbulent regime.

V. ANALYSIS OF FLOW THROUGH MULTISTAGE ECCENTRIC ORIFICE PLATE ASSEMBLIES

The flow through multistage eccentric orifice plate assemblies is analysed over a wide range of parameters, the number of stages considered are 2, 3, 5 and 7. For each case, the spacing between the stages is varied as $(X/D) = 0.5, 1, 2, 3, 4$ and 5. In each case, analysis have been carried out for two diameter ratio namely $\beta = 0.3$ and 0.5 at Reynolds number $Re_D = 10^5$.

Each individual stage consists of an eccentric orifice plate of 1 mm thickness without bevelling. The orifice plates in successive stages are arranged in a staggered fashion (rotated by 180°) so that maximum pressure reduction occurs. The data has been analysed to obtain the discharge coefficient for each stage as well as

overall pressure reduction. The following sections give the details and conclusions drawn from the analysis.

In order to access the efficiency of pressure reduction, the following two additional parameters are defined.

Efficiency factor (R)

Efficiency factor for a multistage orifice plate assembly can be defined as the ratio of summation of pressure drops across each stage to the pressure drop between upstream face of first stage and downstream face of last stage.

It is denoted by 'R' and mathematically represented as,

$$R = \frac{\sum \Delta P_i}{\Delta P} \text{ for } i = [1, 2, 3, \dots, (N - 1), N]$$

Where,

ΔP_i = Pressure differential across i^{th} stage

ΔP = Pressure drop between upstream face of first stage and downstream face of last stage

N = Number of stages

The parameter 'R' represents the efficiency of the pressure reduction. If 'R' is higher than unity, then the overall pressure reduction is higher than that of individual stages obviously, 'R' will be a function of spacing between the stages (X/D) , when multistage orifice plate assemblies is being used as pressure reduction device. It will be desirable to choose the spacing which gives maximum pressure drop.

Pressure Reduction Ratio (PRR)

Pressure reduction ratio for a multistage orifice plate assembly can be defined as the ratio of permanent pressure loss of a multistage to that of a single stage under same flow conditions.

It is denoted by 'PRR' and mathematically represented as,

$$PRR = \frac{[(\Delta P)_{\text{Perm}}]_{\text{Multi Stage}}}{[(\Delta P)_{\text{Perm}}]_{\text{Single Stage}}}$$

$$PRR = \frac{[(\Delta P' - \Delta P'')]_{Multi\ Stage}}{[(\Delta P' - \Delta P'')]_{Single\ Stage}}$$

Where,

$(\Delta P)_{perm}$ = Permanent pressure loss

ΔP^1 = Pressure drop between inlet and outlet of pipe with orifice

ΔP^{11} = Pressure drop between inlet and outlet of pipe without orifice

The parameter 'PRR' represents the pressure reduction for a multistage orifice plate assembly as compared to a single stage orifice plate assembly. It is to be noted that, if there is no interference between the stages then the value of 'PRR' will be numerically equal to the number of stages used. However, this happens only when the spacing between the stages (X/D) is very large. At smaller spacing, it is expected that 'PRR' will be higher than number of stages (N) and the best is that which gives highest value for this parameter.

Terminologies for Multistage Eccentric Orifice Plate Assemblies

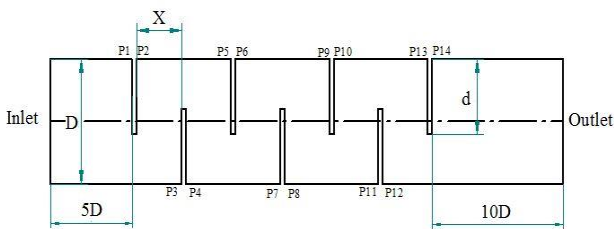


Figure. 5.1: Terminologies for Multistage Eccentric Orifice Plate Assemblies

While analysing the multistage eccentric orifice plate assemblies, the following terminologies are used. The flow domain for multistage eccentric orifice plate assembly is as shown in Fig. 5.1.

At the inlet of the pipe length of 5D and at the outlet of the pipe length of 10D are included.

'P₁' to 'P₁₄' are the pressure at the upstream and downstream of each stage as shown in Fig. 5.1. Thus for the third stage 'P₅' represents the pressure at the upstream corner tap and 'P₆' represents the pressure at the downstream corner tap.

'P_{in}' and 'P_{out}' represents the pressures at inlet and outlet of the pipe respectively with orifice plates.

P_{in}' and P_{out}' represents the pressures at inlet and outlet of the pipe respectively without orifice plates.

$\Delta P_1 = (P_1 - P_2)$ represents the pressure drop across the first stage. Similarly, pressure differentials ΔP_2 to ΔP_7 are defined.

The value of discharge coefficient of ith stage (C_{di}) is calculated from the computed value of respective ΔP_i , where, i = 1 to 7.

Value of the overall discharge coefficient (C_d) is calculated using (ΔP) as the pressure differential. Where, ΔP is the pressure difference between upstream corner tap of first stage and downstream corner tap of the last stage.

The permanent pressure loss coefficient (C_L) is defined as,

$$C_L = \frac{(\Delta P)_{perm}}{\Delta P}$$

Where,

$(\Delta P)_{perm}$ = Permanent pressure loss (Pa)

$\Delta P^1 = (P_{in} - P_{out})$ = Pressure drop between inlet and outlet of pipe with orifice (Pa)

$\Delta P^{11} = (P_{in}^1 - P_{out}^1)$ = Pressure drop between inlet and outlet of pipe without orifice (Pa)

The values of 'R' and 'PRR' are also calculated using the formulae given earlier.

Flow Domain

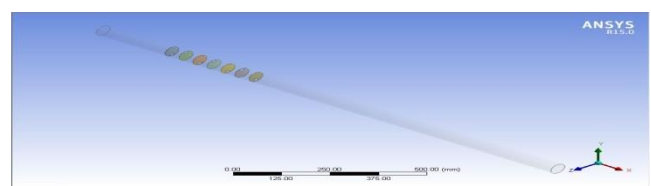


Figure. 5.2: Flow Domain for Multistage Eccentric Orifice Plate Assemblies

Meshing

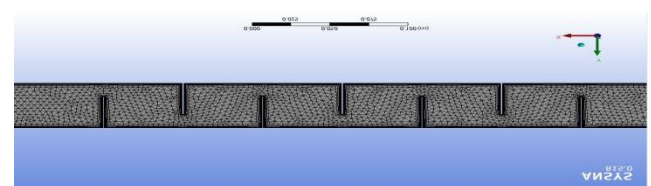


Figure. 5.3: Mesh used for Multistage Eccentric Orifice Plate Assemblies

Range of parameters Studied

CFD analysis have been carried out by considering number of stages varying from 2, 3, 5 and 7 for two diameter ratios namely $\beta = 0.3$ and 0.5 and six spacing ($X/D = 0.5, 1, 2, 3, 4$ and 5) at Reynolds number $Re_D = 10^5$.

Effect of Spacing (X/D) on Characteristics of Multistage Eccentric Orifice Plate Assemblies

In the present section, analysis of flow through multistage eccentric orifice plate assemblies is carried out at different spacing and diameter ratios at Reynolds number $Re_D = 10^5$.

As mentioned before, analyses have been carried out by considering number of stages varying from 2, 3, 5 and 7 for two diameter ratios namely $\beta = 0.3$ and 0.5 and six spacing ($X/D = 0.5, 1, 2, 3, 4$ and 5) at Reynolds number $Re_D = 10^5$. The computed values are tabulated for all the cases in Tables 5.1 (a) to 5.1 (h).

It is observed that, pressure drop across first stage is smaller as compared to that of successive stages. The spacing greatly affects the total pressure drop. The value of discharge coefficient for a last stage is much lower than that of the remaining stages due to strong interference effects.

A careful study of the values tabulated in Tables 5.1(a) to 5.1(h) reveals the following conclusions which are given below.

Table 5.1(a): Effect of (X/D) on characteristics of two stage eccentric orifice plate assemblies with $D = 50$ mm, $Re_D = 10^5$ & $\beta = 0.3$

X/D	0.5	1	2	3	4	5
ΔP_1	352384	523116	594897	612076	61719	617947
ΔP_2	1078506	1211474	1060968	908271	794316	729890
ΔP	1154812	1416353	1366590	1342666	1290662	1258502
ΔP^I	1111259	1368289	1317963	1293895	1243638	1210604
ΔP^{II}	896	896	896	896	896	896
C_{d1}	0.8336	0.6842	0.6416	0.6325	0.6299	0.6295
C_{d2}	0.4765	0.4496	0.4804	0.5192	0.5552	0.5792
C_d	0.4605	0.4158	0.4233	0.4270	0.4356	0.4411
C_L	0.9615	0.9654	0.9637	0.9630	0.9628	0.9612
R	1.2390	1.2246	1.2216	1.1323	1.0935	1.0709
PRR	1.9566	2.4095	2.3208	2.2784	2.1899	2.1317

Table 5.1 (b): Effect of (X/D) on characteristics of two stage eccentric orifice plate assemblies with $D = 50$ mm, $Re_D = 10^5$ & $\beta = 0.5$

X/D	0.5	1	2	3	4	5
ΔP_1	53291	56141	74157	75507	76063	76210
ΔP_2	118069	163142	157364	143942	120013	102613
ΔP	124601	177557	172744	167173	156978	149171
ΔP^I	115351	161305	155842	150353	141351	133436
ΔP^{II}	896	896	896	896	896	896
C_{d1}	0.7503	0.7310	0.6360	0.6303	0.6280	0.6274
C_{d2}	0.5040	0.4288	0.4366	0.4565	0.4999	0.5407
C_d	0.4906	0.4110	0.4167	0.4236	0.4371	0.4484
C_L	0.9185	0.9034	0.8969	0.8940	0.8937	0.8885
R	1.3752	1.3597	1.3402	1.3127	1.2490	1.1987
PRR	1.9509	2.7342	2.6411	2.5475	2.3941	2.2592

Table 5.1 (c): Effect of (X/D) on characteristics of three stage eccentric orifice plate assemblies with $D = 50$ mm, $Re_D = 10^5$ & $\beta = 0.3$

X/D	0.5	1	2	3	4	5
ΔP_1	356967	514996	597918	612312	630291	626121
ΔP_2	911058	1156538	1032242	908168	841328	741433
ΔP_3	774558	1232228	965242	822261	762562	713441
ΔP	1680404	2255229	2125023	2036895	1989659	1906570
ΔP^I	1633866	2204549	2074915	1989289	1941122	1858965
ΔP^{II}	881	881	881	881	1002	1002
C_{d1}	0.8283	0.6896	0.6400	0.6324	0.6233	0.6254
C_{d2}	0.5184	0.4601	0.4870	0.5193	0.5395	0.5747
C_{d3}	0.5623	0.4458	0.5037	0.5457	0.5667	0.5859
C_d	0.3817	0.3295	0.3394	0.3467	0.3508	0.3584
C_L	0.9717	0.9771	0.9760	0.9761	0.9751	0.9745
R	1.2155	1.2875	1.2213	1.1501	1.1228	1.0914
PRR	2.8775	3.8832	3.6547	3.5039	3.4188	3.2740

Table 5.1 (d): Effect of (X/D) on characteristics of three stage eccentric orifice plate assemblies with $D = 50$ mm, $Re_D = 10^5$ & $\beta = 0.5$

X/D	0.5	1	2	3	4	5
ΔP_1	18204	53925	73653	75182	76167	760780
ΔP_2	107165	153892	154451	143362	120461	103060
ΔP_3	102498	164979	146306	111903	99370	90968
ΔP	207488	284866	266387	242829	230001	217197
ΔP^I	193392	267601	249352	227007	214200	201273
ΔP^{II}	881	881	881	881	1001	1001
C_{d1}	1.2837	0.7458	0.6382	0.6316	0.6275	0.6279
C_{d2}	0.5290	0.4415	0.4407	0.4574	0.4990	0.5395
C_{d3}	0.5410	0.4264	0.4528	0.5177	0.5494	0.5742
C_d	0.3802	0.3245	0.3355	0.3514	0.3611	0.3716
C_L	0.9278	0.9362	0.9327	0.9312	0.9269	0.9220
R	1.0982	1.3086	1.4055	1.3608	1.2869	1.2436
PRR	3.2814	4.5463	4.2352	3.8544	3.6340	3.4137

Table 5.1 (e): Effect of (X/D) on characteristics of five stage eccentric orifice plate assemblies with $D = 50$ mm, $Re_D = 10^5$ & $\beta = 0.3$

X/D	0.5	1	2	3	4	5
ΔP_1	350710	519221	594949	612114	616255	617409
ΔP_2	899011	1161383	1034258	905320	798308	730806
ΔP_3	572794	1158337	933960	813917	741956	704254
ΔP_4	603888	1190185	928807	818170	736871	689936
ΔP_5	781875	1277160	961044	828989	747118	696205
ΔP	2679417	3957923	3614857	3435922	3255542	3141945
ΔP^I	2634467	3907888	3565646	3388418	3207890	3094397
ΔP^{II}	1056	1056	1056	1056	1519	1519
C_{d1}	0.8356	0.6860	0.6416	0.6325	0.6304	0.6298
C_{d2}	0.5219	0.4592	0.4866	0.5201	0.5538	0.5789
C_{d3}	0.6538	0.4598	0.5120	0.5485	0.5745	0.5897
C_{d4}	0.6368	0.4536	0.5135	0.5471	0.5765	0.5958
C_{d5}	0.5596	0.4379	0.5048	0.5435	0.5725	0.5931
C_d	0.3023	0.2487	0.2602	0.2669	0.2742	0.2791
C_L	0.9828	0.9870	0.9860	0.9858	0.9848	0.9843
R	1.1973	1.3406	1.2318	1.1579	1.1182	1.0944
PRR	4.6405	6.8844	6.2814	5.9691	5.6501	5.4501

Table 5.1 (f): Effect of (X/D) on characteristics of five stage eccentric orifice plate assemblies with D = 50 mm, $Re_D = 10^5$ & $\beta = 0.5$

X/D	0.5	1	2	3	4	5
ΔP_1	18467	53930	74368	75560	76148	76205
ΔP_2	106675	154286	154576	141937	120800	103195
ΔP_3	67980	148878	142402	114457	99129	91328
ΔP_4	96121	173412	140309	112279	98299	91029
ΔP_5	122557	192930	141824	112756	98929	91699
ΔP	371179	512582	452476	405749	374914	355530
ΔP^I	357489	494724	435806	389487	359175	339327
ΔP^{II}	1056	1056	1056	1056	1519	1519
C_{d1}	1.2745	0.7458	0.6351	0.6301	0.6276	0.6274
C_{d2}	0.5303	0.4409	0.4405	0.4597	0.4983	0.5391
C_{d3}	0.6643	0.4488	0.4589	0.5119	0.5501	0.5731
C_{d4}	0.5586	0.4159	0.4624	0.5169	0.5524	0.5740
C_{d5}	0.4947	0.3943	0.4599	0.5158	0.5506	0.5719
C_d	0.2842	0.2419	0.2574	0.2719	0.2828	0.2904
C_L	0.9602	0.9630	0.9608	0.9573	0.9539	0.9501
R	1.1094	1.4113	1.4442	1.3727	1.3157	1.2754
PRR	6.0755	8.4147	7.4105	6.6209	6.0963	5.7580

Table 5.1 (g): Effect of (X/D) on characteristics of seven stage eccentric orifice plate assemblies with D = 50 mm, $Re_D = 10^5$ & $\beta = 0.3$

X/D	0.5	1	2	3	4	5
ΔP_1	360693	523063	596407	612668	616253	615593
ΔP_2	908995	1170024	1038919	898836	789719	724636
ΔP_3	587499	1153024	945385	817437	743236	699051
ΔP_4	616604	1189347	921880	813730	735278	687635
ΔP_5	587908	1204180	936693	811712	744022	698132
ΔP_6	599990	1189706	927781	819994	734818	690963
ΔP_7	778582	1258061	961751	824632	748887	704525
ΔP	3716165	5619147	5102144	4814090	4558205	4380501
ΔP^I	3671410	5567882	5052384	4764760	4510109	4333970
ΔP^{II}	1291	1291	1291	1291	1775	1775
C_{d1}	0.8240	0.6842	0.6408	0.6322	0.6304	0.6307
C_{d2}	0.5190	0.4575	0.4855	0.5219	0.5568	0.5813
C_{d3}	0.6456	0.4608	0.5089	0.5473	0.5740	0.5919
C_{d4}	0.6302	0.4537	0.5154	0.5486	0.5771	0.5967
C_{d5}	0.6454	0.4509	0.5113	0.5492	0.5737	0.5922
C_{d6}	0.6389	0.4537	0.5137	0.5465	0.5773	0.5953
C_{d7}	0.5608	0.4412	0.5046	0.5490	0.5718	0.5896
C_d	0.2567	0.2087	0.2190	0.2255	0.2317	0.2364
C_L	0.9870	0.9906	0.9899	0.9894	0.9890	0.9889
R	1.1948	1.5074	1.2404	1.1630	1.1215	1.1004
PRR	6.4673	9.8092	8.9008	8.3940	7.9444	7.6340

Table 5.1 (h): Effect of (X/D) on characteristics of seven stage eccentric orifice plate assemblies with D = 50 mm, $Re_D = 10^5$ & $\beta = 0.5$

X/D	0.5	1	2	3	4	5
ΔP_1	16404	54150	74383	75969	76012	75822
ΔP_2	109196	153937	154171	143420	120561	101866
ΔP_3	74226	150044	143824	115251	99178	91797
ΔP_4	97674	171691	141514	113297	98569	90867
ΔP_5	91510	175539	141170	113368	99714	92226
ΔP_6	96056	177069	141713	113722	98699	91483
ΔP_7	125925	199086	145755	113923	100006	91507
ΔP	541654	740534	638949	567603	520458	492010
ΔP^I	528254	722753	622114	551306	505119	476196
ΔP^{II}	1291	1291	1291	1291	1775	1775
C_{d1}	1.3523	0.7443	0.6350	0.6284	0.6282	0.6290
C_{d2}	0.5241	0.4414	0.4411	0.4573	0.4988	0.5426
C_{d3}	0.6357	0.4471	0.4567	0.5101	0.5499	0.5716
C_{d4}	0.5542	0.4180	0.4604	0.5145	0.5516	0.5745
C_{d5}	0.5725	0.4134	0.4609	0.5144	0.5485	0.5703
C_{d6}	0.5588	0.4116	0.4601	0.5136	0.5513	0.5726
C_{d7}	0.4880	0.3881	0.4536	0.5131	0.5477	0.5725
C_d	0.2353	0.2012	0.2166	0.2299	0.2400	0.2469
C_L	0.9728	0.9742	0.9716	0.9690	0.9671	0.9642
R	1.1280	1.4604	1.4751	1.3899	1.3252	1.2917
PRR	8.9823	12.2976	10.5821	9.3752	8.5797	8.0867

Major Conclusions

The analysis described in this section on the characteristics of multistage eccentric orifice plate assemblies have brought out the effect of different design parameters on the pressure reduction capacity. The following broad conclusions can be drawn from this analysis.

- The optimum spacing (X/D) for achieving maximum pressure reduction is found to be (X/D) = unity. This is valid for all number of stages in the range 2 to 7 and also at two diameter ratios analyzed $\beta = 0.3$ and 0.5 .
- At the optimum spacing, the total pressure reduction is always higher than sum of individual pressure drops across each stages.
- The pressure reduction ratio at the optimum spacing is always larger than number of stages.
- The efficiency factor (R) also shows a maximum at (X/D) = 1 and it is always larger than unity.
- The discharge coefficient of intermediate stages in multistage eccentric orifice plate assemblies is more or less same. However, this value is lower than that of individual single orifice plate.
- The characteristics of the multistage eccentric orifice plate assemblies (C_d , C_L , PRR and R) are relatively unaffected by the Reynolds number in the fully turbulent regime ($Re_D > 10^3$).

VI. Effect of Number of Stages on Characteristics of Multistage Eccentric Orifice Plate Assemblies

In the present study, CFD has been used to analyse the flow through multistage eccentric orifice plate assemblies with number of stages in the range 2 to 7. In order to have a comparative study of the effect of number of stages, the computed results are analysed in terms of this parameters.

A. Effect of Number of Stages on the overall Characteristics of the Multistage Eccentric Orifice Plate Assemblies

Figs. 6.1 (a) and 6.1 (b) show the variation of overall discharge coefficient (C_d) with (X/D) for two diameter ratios $\beta = 0.3$ and $\beta = 0.5$ respectively. It is observed that at any (X/D), the values of overall discharge

coefficient (C_d) decreases with increasing number of stages at both diameter ratios. Further, for all stages the value of discharge coefficient (C_d) is minimum at $(X/D) = 1$ showing that it is the optimum spacing.

Figs. 6.2 (a) and 6.2 (b) show the effect of spacing on the values of PRR for two diameter ratios $\beta = 0.3$ and $\beta = 0.5$ respectively. As the number stages increases at any given spacing (X/D) , the value of PRR also increases. Again at $(X/D) = 1$, PRR is maximum for number of stages and diameter ratios.

The variation of efficiency factor 'R' with (X/D) is shown in Figs. 6.3 (a) and 6.3 (b) for two diameter ratios $\beta = 0.3$ and $\beta = 0.5$ respectively. At $(X/D) = 1$ and $\beta = 0.3$, a sharp peak is observed. The efficiency factor is always higher than unity showing higher pressure reduction across each stage due to interference effects. The mechanism of pressure reduction is optimum at $(X/D) = 1$.

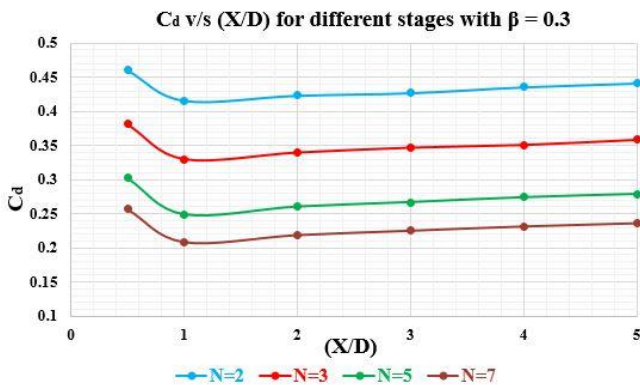


Figure. 6.1 (a): Variation of C_d with (X/D) for multi stage eccentric orifice plate assemblies at $Re_D=10^5$ & $\beta = 0.3$

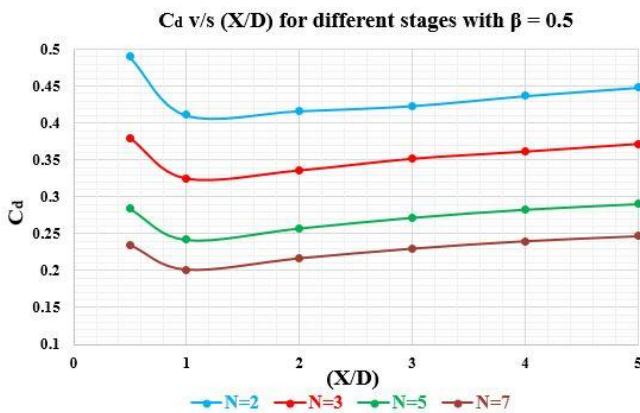


Figure. 6.1 (b): Variation of C_d with (X/D) for multi stage eccentric orifice plate assemblies at $Re_D=10^5$ & $\beta = 0.5$

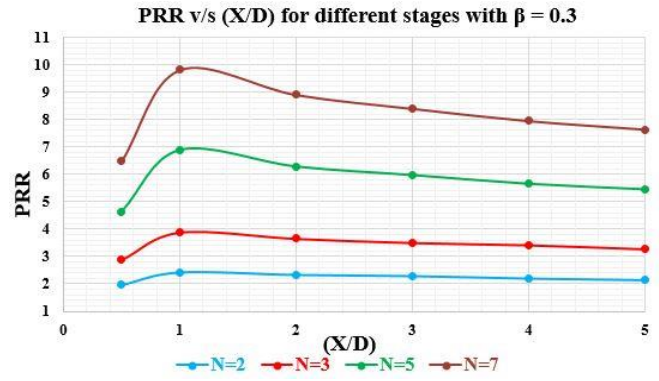


Figure. 6.2 (a): Variation of PRR with (X/D) for multi stage eccentric orifice plate assemblies at $Re_D=10^5$ & $\beta = 0.3$

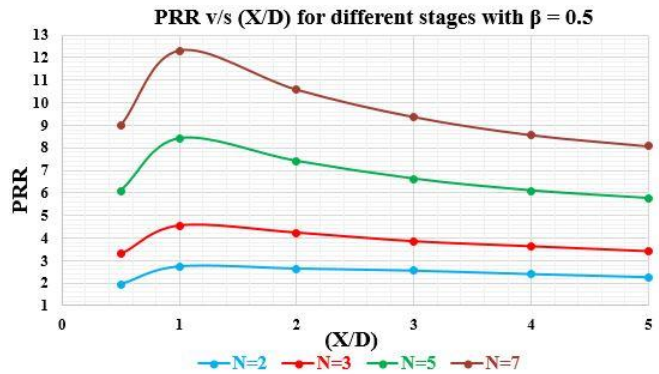


Figure. 6.2 (b): Variation of PRR with (X/D) for multi stage eccentric orifice plate assemblies at $Re_D=10^5$ & $\beta = 0.5$

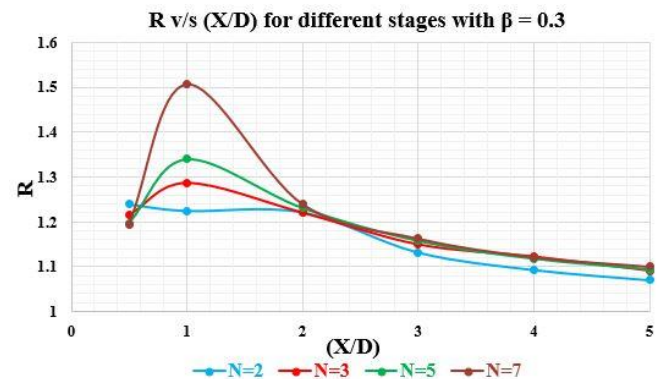


Figure. 6.3 (a): Variation of R with (X/D) for multi stage eccentric orifice plate assemblies at $Re_D=10^5$ & $\beta = 0.3$

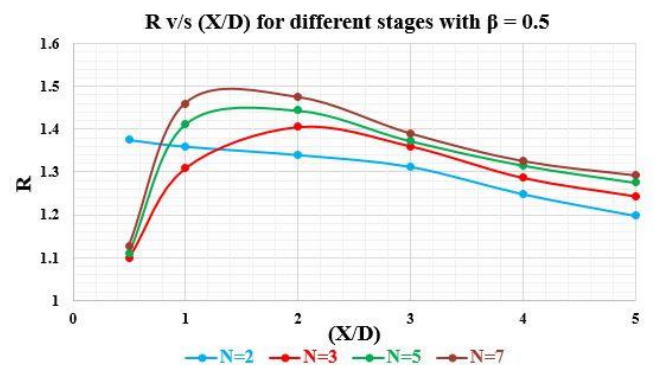


Figure. 6.3 (b): Variation of R with (X/D) for multi stage eccentric orifice plate assemblies at $Re_D=10^5$ & $\beta = 0.5$

B. Effect of Number of Stages on Pressure Reduction Ratio of Eccentric Orifice Plate Assemblies with $(X/D) = 1$ and $Re_D = 10^5$

The variation of pressure reduction ratio 'PRR' with number of stages for two diameter ratios $\beta = 0.3$ and $\beta = 0.5$ at spacing of $(X/D) = 1$ is plotted in Figs. 6.4 (a) and 6.4 (b) respectively. It shows that the variation is close to linear. However, the values of 'PRR' is always larger than number of stages (N). This data is very useful for the designer of multistage eccentric orifice plate assemblies.

From the linear curve fitting equation obtained from the Fig. 6.4 (a), at optimum spacing of $(X/D) = 1$ and for diameter ratio $\beta = 0.3$, if the number of stages (N) are known then the value of 'PRR' can be numerically calculated using the equation

$$PRR = 1.4682N - 0.4682$$

From the linear curve fitting equation obtained from the Fig. 6.4 (b), at optimum spacing of $(X/D) = 1$ and for diameter ratio $\beta = 0.5$, if the number of stages (N) are known then the value of 'PRR' can be numerically calculated using the equation

$$PRR = 1.8829N - 0.8829$$

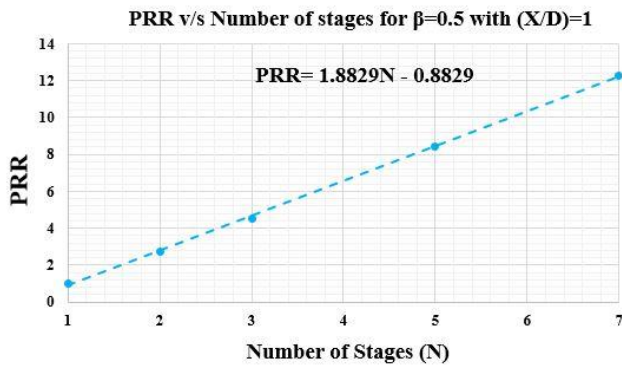


Figure. 6.4 (a): Variation of PRR with Number of stages at $Re_D = 10^5$, $(X/D) = 1$ & $\beta = 0.3$

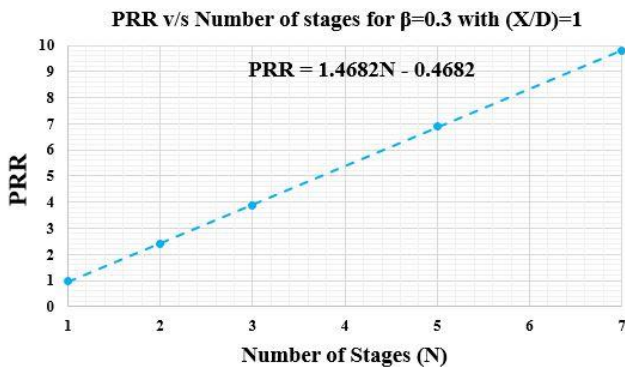


Figure. 6.4 (b): Variation of PRR with Number of stages at $Re_D = 10^5$, $(X/D) = 1$ & $\beta = 0.5$

VII. CONCLUDING REMARKS

The specific conclusions drawn from different aspects of study have already given in the discussion part of each chapter. Hence, only broad general conclusions are given here.

- A validated CFD methodology can be used to accurately analyse the flow through multistage eccentric orifice plate assemblies. However, it is important to ensure proper meshing near the wall as well as a most suitable turbulence model. The values of non-dimensional distance from the wall (y^+) for the wall adjacent elements should be in the range of unity. K- ϵ Standard turbulence model with a scalable wall functions is found to be suitable for this class of problems.
- The methodology developed is validated by analyzing the flow through standard concentric orifice plate considering it as a three dimensional steady incompressible flow.
- Detail analysis of flow through single stage eccentric orifice plate assemblies has demonstrated that CFD can be used to accurately predict its characteristics both within and outside the range specified by BS 1042 [2].
- A spacing of is found to be optimum for achieving maximum pressure reduction in multistage eccentric orifice plate assemblies.
- In multistage eccentric orifice plate assemblies, at the optimum spacing of $(X/D) = 1$, the overall pressure reduction is always higher than the pressure reduction based on individual stage values.

VIII. SCOPE FOR FUTURE WORK

The present work is limited to incompressible Newtonian fluid, temperature and compressibility effects are not considered. Thus, the work can be extended to include the following aspects.

- The fluid can be considered as compressible with thermal effects and the phenomenon of choking can also be analyzed.
- The effect of thicker orifice plates on the characteristics of multistage eccentric orifice plate assemblies should be studied.
- The analysis can be extended to multiple-hole orifice plates placed in staggered positions.
- The analysis of noise and vibrations in these devices can be studied.

IX. REFERENCES

- [1]. Bureau of Indian Standards, "IS 14615 (Part 1), ISO 5167-1:1999", Measurement of Fluid Flow by Means of Pressure Differential Devices, New Delhi.
- [2]. British Standards Institution, "BS 1042: Section 1.2:1989", Measurement of Fluid Flow in Closed Conduits, Specification for Square-Edged Orifice Plates and Nozzles (With Drain Holes, In Pipes below 50 mm Diameter, as Inlet and Outlet Devices) and Other Plates.
- [3]. R K Singh, S N Singh and Dr. V. Seshadri. Performance Evaluation of Orifice Plate Assemblies under Non-Standard Conditions Using CFD. Indian Journal of Engineering & Material Sciences. Volume-17, December 2010, pp. 397-406.
- [4]. Karthik G.S, Yogesh Kumar K J, Dr. V. Seshadri. Prediction of Performance Characteristics of orifice Plate Assembly for Non-Standard Conditions Using CFD. International Journal of Engineering and Technical Research (IJETR). ISSN: 2321-0869, Volume-3, Issue-5, May 2015, pp.162-167.
- [5]. Abdulrazaq A. Araoye, Hasan M. Badr, Wael H. Ahmed. Dynamic Behaviour of Flow through Multi-Stage Restricting Orifices. Proceedings of the 3rd International Conference on Fluid Flow, Heat and Mass Transfer (FFHMT'16). Ottawa, Canada-May 2-3, 2016. pp. 161.
- [6]. Mohan Kumar H M, Yogesh Kumar K J, Dr. V. Seshadri. CFD Analysis of Flow through Dual Orifice Plate Assembly. International Journal of Emerging Technology and Advanced Engineering. ISSN: 2250-2459, Volume-5, Issue-10, October 2015, pp.136-144.
- [7]. Lakshmisha H R, Dr. V. Seshadri, Puneeth Kumar S B. Numerical Analysis of Flow through Multi-Stage Orifice Plate Assemblies with Alternate Concentric and Annular Orifice Plates. International Journal of Modern Trends in Engineering and Research. ISSN: 2393-8161, Volume-3, Issue-9, September 2016. pp. 47-56.
- [8]. D Zaheriea. Numerical Analysis of Eccentric Orifice Plate Using ANSYS Fluent Software. International Engineering Research and Innovation Symposium (IRIS). IOP Conf. Series: Material Science and Engineering 160 (2016) 012041. doi: 10.1088/1757-899X/160/012041. pp. 1-6.
- [9]. Andrej Lipej, Rok Pavlin, Aljiz Skerlavaj, Bogdon Jancer, Matjaz Cernec. Numerical and Experimental Design of Multi-Stage Orifice FWRO-004. 22nd International Conference on Nuclear Energy for New Europe (NENE). Bled-Slovenia, September 9-12. pp. 229.1-229.8.
- [10]. Malatesh Barki, Ganesha T, Dr. M C Math. CFD Analysis and Comparison of Fluid Flow through A Single Hole and Multi Hole Orifice Plate. International Journal of Research in Advent Technology. ISSN: 2321-9637, Volume-2, Issue-8, August 2014. pp. 6-15.
- [11]. H K Versteeg and W Malalasekara, "An Introduction to Computational Fluid Dynamics, The Finite Volume Method", Second Edition, Pearson Education, Ltd. (2007).